Competitive Vaporization and Decomposition of Liquid RDX

Gregory T. Long, Sergey Vyazovkin, Brittany A. Brems, and Charles A. Wight*

Center for Thermal Analysis, Department of Chemistry, University of Utah, 315 S. 1400 E., Salt Lake City, Utah 84112

The thermal decomposition of hexahydro-1,3,5-trinitro-1,3,5-triazine (RDX) has been studied by thermogravimetric analysis (TGA) and differential scanning calorimetry (DSC). Activation energies as a function of the extent of conversion, α, have been determined by model-free isoconversional analysis of these data. In open pans, evaporation is a prevalent process with an activation energy of $\sim$100 kJ mol^{-1}. Confining the system in either a pierced pan or a closed pan promotes liquid state decomposition of RDX that occurs with an activation energy of $\sim$200 kJ mol^{-1}, which suggests scission of an N−N bond as the primary decomposition step. In such a confined environment, gas phase decomposition is a competing channel with an activation energy estimated to be $\sim$140 kJ mol^{-1}. In a closed pan, RDX generates a heat release of $\sim$500 kJ mol^{-1} that is independent of both the heating rate, β, and the mass.

Introduction

The widespread commercial and military use of explosives has prompted a vigorous effort to measure the kinetics and elucidate the mechanism of their decomposition.[1,2] Both explosive decomposition that occurs under rapid thermal or mechanical insult and the cook-off chemistry that leads to decomposition during slow heating are of considerable interest. Fast heating techniques such as thin film laser pyrolysis,[3−5] laser pyrolysis MS,[6] T-jump FTIR,[7] and SMATCH (simultaneous mass and temperature change) FTIR[8,9] probe decomposition under conditions close to those of combustion. Slow heating techniques such as thermogravimetric analysis (TGA), and differential scanning calorimetry (DSC) interrogate the slow cook-off chemistry and the findings can lead to the safer manufacture, handling, and storage of explosives.[1]

Despite the apparent simplicity of pure explosives, their decompositions usually demonstrate an intricate interplay of multiple step processes that occur in both the gas and condensed phases. Individual steps are likely to have different activation energies, and it would be anticipated that the relative contributions of each step to the overall decomposition rate measured by TGA or DSC will vary with temperature and the extent of conversion. For this reason, the effective activation energy would also likely be a function of temperature and/or extent of conversion. However, this effect can easily be overlooked when using standard model fitting methods that are designed to extract a single activation energy for an entire process.[10,11] A model-free approach to kinetic analysis[12,13] allows the extraction of realistic kinetic information from overall rate measurements. This approach applies the isoconversional method to yield activation energies as a function of the extent of conversion and reflects the variation in the relative contributions of single reaction steps to the overall reaction rate measured by TGA and DSC.[12,13] Such information assists in detecting multistep kinetics and in elucidating reaction mechanisms.[12,13] The isoconversional method has been successfully applied to several energetic materials including ammonium perchlorate (AP),[11]

ammonium dinitramide (ADN),[10,14,15] octahydro-1,3,5,7-tetranitro-1,3,5,7-tetrazocine (HMX),[11] and hydroxy-terminated polybutadiene (HTPB) and polybutadiene−acrylonitrile (PBAN) propellants.[16] In this paper, the isoconversional method has been applied to study the kinetics of vaporization and decomposition of liquid state hexahydro-1,3,5-trinitro-1,3,5-triazine (RDX). Although the activation energies for the liquid state decomposition of RDX have been reported in a number of studies[17−26] (Table 1), none of them addresses the dependence of the activation energy on the extent of conversion, either under an assumption of first-order kinetics or by using Kissinger's method.[27]

Experimental Section

RDX, obtained from the Army Research Laboratories, Aberdeen Proving Grounds, MD, was studied as a granular powder without further purification.

TGA experiments were performed on a Mettler-Toledo TGA/SDTA851 module. The "open pan" experiments were performed on $\sim$1 mg RDX samples, which were placed in open 40 μL Al pans. The "pierced pan" experiments were conducted with $\sim$0.5 mg samples, which were placed in a 40 μL Al pan and covered with a piercing Al lid. Immediately before the experiment, 1 mm holes were pierced by using an automatic piercing device. Both open and pierced pan experiments were carried out at heating rates of β = 7.5, 10.0, 12.5, 15.0, 17.5, and 20.0 °C min^{-1} over a temperature range of 25−300 °C. N$_2$ was used as the carrier gas at a flow rate of 70 mL min^{-1}.

DSC curves were collected on a Mettler-Toledo DSC821 module. Samples for open and pierced pan experiments were prepared as previously described. 40 μL Al pans were used in open, pierced, and closed pan experiments. N$_2$ carrier gas flowed at a rate of 80 mL min^{-1}. Open pan experiments on RDX samples of $\sim$1 mg were conducted at heating rates of β = 7.5, 10.0, 12.5, 15.0, 17.5, and 20.0 °C min^{-1} for temperatures of 25−300 °C. Pierced pan experiments were performed with sealed Al piercing lids on $\sim$0.5 mg samples of RDX using a 1.0 mm piercer and at the same heating rates as in open pans. For closed pan experiments, small samples ($\leq$120 μg) were

* Corresponding author. E-mail: wight@chemistry.utah.edu.

Vaporization and Decomposition of Liquid RDX

J. Phys. Chem. B, Vol. 104, No. 11, 2000 **2571**

TABLE 1: Activation Energies for the Thermal Decomposition of Liquid RDX

E_α/kJ mol^{-1}	evaluated by equation	experiment	ref
199	1st-order reaction	isothermal manometry	17
190	?[a]	isothermal manometry	18
282	0th-order reaction	nonisothermal DSC	19
204	1st-order reaction	isothermal GC	20
189	1st-order reaction	nonisothermal DSC	21
180[b]	1st-order reaction	isothermal DSC	22
88[c]	Clausius−Clapeyron	isothermal DSC	22
197	1st-order reaction	isothermal DSC	23
171	see ref 24	isothermal DSC	24
176	see refs 24, 25	nonisothermal DSC	24, 25
176	Kissinger	nonisothermal DSC	24
125	Kissinger	nonisothermal DSC	24
199	Kissinger	nonisothermal DTA	26
200	1st-order reaction	isothermal TGA	26

[a] Not reported. [b] The value was corrected in ref 23 as 197 kJ mol^{-1}. [c] Assigned to vaporization.

sealed under N$_2$ in crimp-sealed standard pans with standard Al lids. Samples were heated at β = 2.5, 5.0, 7.5, 10.0, 12.5, 15.0, 17.5, and 20.0 °C min^{-1} for temperatures of 25−300 °C.

Kinetic Analysis. The kinetics of heterogeneous decompositions are traditionally described by the basic kinetic equation[28]

$$d\alpha/dt = k(T)\,f(\alpha) \tag{1}$$

where α represents the extent of reaction ($\alpha = 0-1$), t is time, $k(T)$ is the rate constant, and $f(\alpha)$ is the reaction model which describes the dependence of the reaction rate on the extent of reaction. The value of α is experimentally determined from TGA traces as a relative mass loss and from DSC traces as a fractional peak area. In most cases, the temperature dependence of $k(T)$ can be satisfactorily described by the Arrhenius equation, whose substitution into eq 1 yields

$$\frac{d\alpha}{dt} = A\,\exp\!\left(\frac{-E}{RT}\right)\!f(\alpha) \tag{2}$$

where E is the activation energy and A is the preexponential factor.

To evaluate the dependence of the effective activation energy on the extent of conversion, we used an advanced isoconversional method,[29] which is based on the assumption that the reaction model is independent of the heating program, $T(t)$. According to this method, for a set of n experiments carried out at different heating programs, the activation energy is determined at any particular value of α by finding E_α that minimizes the function

$$\Phi(E_\alpha) = \sum_{i=1}^{n}\sum_{j\neq i}^{n}\frac{J[E_\alpha,T_i(t_\alpha)]}{J[E_\alpha,T_j(t_\alpha)]} \tag{3}$$

Henceforth, the subscript α denotes the values related to a given extent of conversion. In eq 3, the integral

$$J[E_\alpha,T_i(t_\alpha)] \equiv \int_0^{t_\alpha}\exp\!\left[\frac{-E_\alpha}{RT_i(t)}\right]\!dt \tag{4}$$

is evaluated numerically for a set of experimentally recorded heating programs, $T_i(t)$. The minimization procedure is repeated for each value of α to find the dependence of the activation energy on the extent of conversion. An advantage of the advanced isoconversional method is that it can be applied to
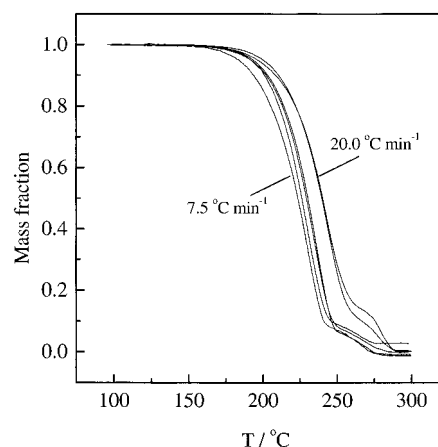
Figure 1. Open pan TGA curves for samples of RDX collected at heating rates of β = 7.5, 10.0, 12.5, 15.0, 17.5, and 20.0 °C min^{-1}.
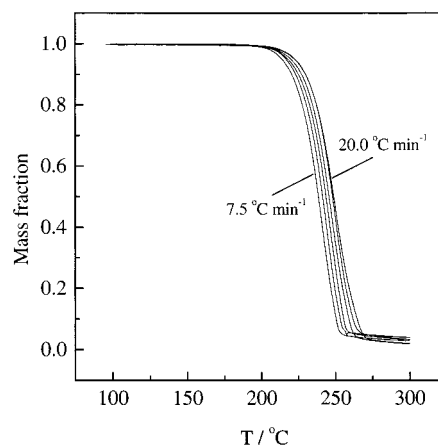
Figure 2. Pierced pan TGA traces for RDX samples acquired at heating rates of β = 7.5, 10.0, 12.5, 15.0, 17.5, and 20.0 °C min^{-1}.

study the kinetics for arbitrary temperature programs (e.g., under a linear heating program distorted by self-heating).[29]

Results

Thermogravimetric Analysis. TGA curves for open pan experiments exhibit a two step mass loss that approaches 100% of the initial mass (Figure 1). The major mass loss during the first step occurs between 170 and 260 °C; the second step takes place between 240 and 290 °C and includes around 10% of the mass loss. Application of the isoconversional method to the TGA data collected for β = 7.5−20.0 °C min^{-1} yields an E_α versus α dependence that shows a fairly constant activation energy of ~100 kJ mol^{-1} for α < 0.7 and corresponds to the first step of mass loss; between 0.7 < α ≤ 0.9, E_α decreases to ~45 kJ mol^{-1} before increasing to ~100 kJ mol^{-1} for α = 0.98 and applies to the second step of mass loss (Figure 4).

Pierced pan experiments yield TGA traces that display a single step of mass loss that exceeds 95% of the initial mass and which occurs over temperatures of 210−270 °C (Figure 2). As compared to the TGA curves corresponding to open pan experiments, the respective TGA curves for pierced pan experiments are shifted to higher temperatures by ~20 °C. The application of the isoconversional method to the traces in Figure 2 leads to an E_α dependence that shows a fairly constant activation energy of ~180 kJ mol^{-1} for 0.1 < α < 0.6, followed by a decrease to ~100 kJ mol^{-1} (Figure 4).

Differential Scanning Calorimetry. A typical DSC curve collected in an open pan for β = 10.0 °C min^{-1} is shown in
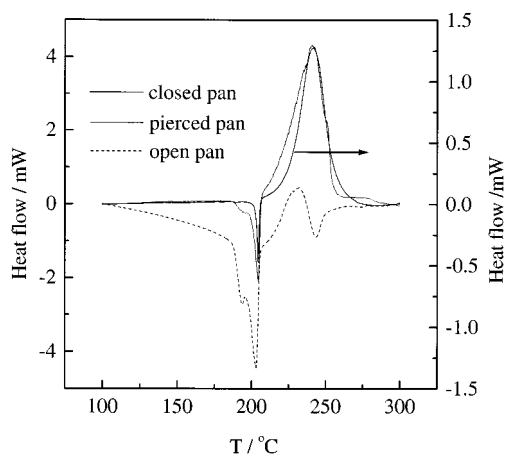
Figure 3. An overlay of DSC curves collected for RDX decomposition in open ($m = 1.263$ mg), pierced ($m = 0.478$ mg), and closed ($m = 0.046$ mg) pans at a heating rate of 10.0 °C min^{-1}.
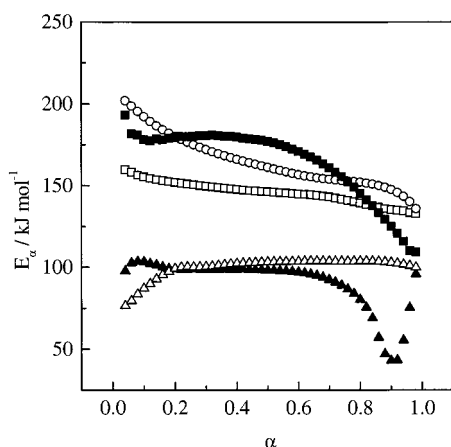

Figure 4. E_α dependencies obtained for TGA (solid symbols) and DSC (open symbols) experiments performed in open (triangles), pierced (squares), and closed (circles) pans.

Figure 3. The common thermal feature in all the open pan DSC curves is a structured endotherm that appears between 180 and 210 °C; it contains a strongly temperature dependent, smaller feature at lower temperature and a much sharper, larger magnitude feature at higher temperature with a peak at 204 °C. At heating rates of 7.5 °C min^{-1} and higher an exotherm occurs between 205 and 255 °C. The application of the isoconversional method to the exotherm for $\beta = 7.5-20.0$ °C min^{-1} gives an E_α dependence with a practically constant activation energy of $E_\alpha \sim 100$ kJ mol^{-1} for $0.2 < \alpha < 1.0$ (Figure 4).

When run in a pierced pan the same features appear in DSC traces. However, the first smaller endotherm becomes even smaller as compared to the second sharp endotherm at 204 °C. The size of the exotherm increases relative to the endotherm as shown for $\beta = 10.0$ °C min^{-1} in Figure 5a. Analyzing the exotherm by the isoconversional method leads to an E_α dependence that shows a small decrease in E_α from ~ 160 kJ mol^{-1} at $\alpha = 0.02$ to ~ 135 kJ mol^{-1} at $\alpha = 0.98$ (Figure 4).

Confining an RDX sample in a closed pan causes a complete disappearance of the first smaller endotherm, whereas the second endotherm again occurs at 204 °C. The size of the normalized exotherm increases as compared to that observed in pierced pan experiments (Figure 5a). Applying the isoconversional method to the exotherm in DSC traces results in an E_α dependence that gradually decreases from $E_\alpha \sim 200$ kJ mol^{-1} at $\alpha = 0.02$ to ~ 135 kJ mol^{-1} at $\alpha = 0.98$ (Figure 4).
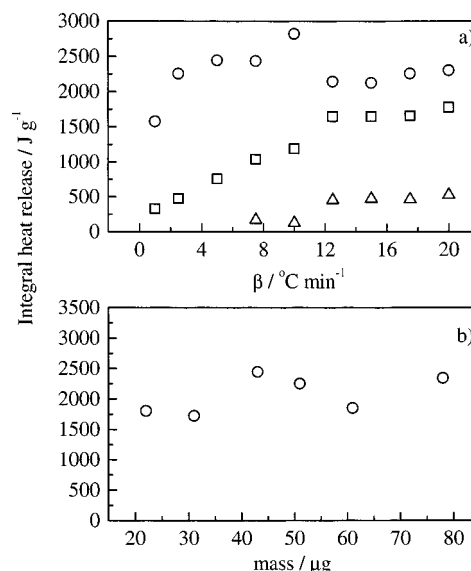
Figure 5. (a) A plot of the integrated and normalized decomposition exotherm of a nonisothermal DSC trace for RDX in a pierced pan (□) and sealed in a closed pan under N$_2$ (○) as a function of β. (b) Plot of the integrated and normalized heat release for the decomposition exotherm from DSC traces of closed pan RDX samples sealed under N$_2$ (○) as a function of sample mass at a heating rate of $\beta = 5.0$ °C min^{-1}.

Figure 5a shows that the integrated and normalized heat release of the exotherm in DSC traces increases as a function of β in both open and pierced pan experiments. In open pan experiments, the maximum total heat release is around 500 J g^{-1}. In pierced pan experiments, the overall heat release increases for $\beta \leq 12.5$ °C min^{-1} after which it approaches an asymptotic value of ~ 1750 J g^{-1}. Closed pan experiments demonstrate a virtually constant heat release of ~ 2250 J g^{-1} that is largely independent of β and of the sample mass (Figure 5).

Discussion

Differential Scanning Calorimetry. The first endotherm is most prominent in open pan experiments, becomes smaller in pierced pan experiments, and disappears in closed pan experiments. This endotherm occurs below the melting point of RDX, reported as 204 °C,[30] and is likely associated with the sublimation of RDX. The second sharper endotherm at 204 °C is invariably observed in all types of DSC experiments and assigned to the melting of RDX (Figure 3). The DSC traces in Figure 3 show that confining RDX in pierced and especially closed pans affects the overall kinetics. First, the decrease in size of the first endotherm in pierced pan and its disappearance in closed pan experiments likely results from an increase in pressure in this confined environment that suppresses sublimation. Second, the trapping of gases in a pan promotes further decomposition as shown by an exotherm that increases in size with increasing confinement.

The occurrence of the exotherm above 204 °C is consistent with the decomposition of liquid RDX. Moreover, the increasing size of the exotherm in going from open to pierced to closed pans indicates that decomposition dominates in more confined environments and that an additional competing endothermic process becomes more important under more open conditions. This competing process is most likely the vaporization of RDX (vide infra). However, as shown in Figure 3, decomposition is sufficiently exothermic to offset endothermic vaporization so that an exotherm is detected even in open pan DSC experiments.

Vaporization and Decomposition of Liquid RDX

J. Phys. Chem. B, Vol. 104, No. 11, 2000 **2573**

Further support of an alternative channel is provided by a heat release that increases with the heating rate and observed for both open and pierced pan experiments (Figure 5). This increase shows that the dominant process at lower heating rates has a lower activation energy than the process that is favored at higher heating rates. An increase in heating rate causes the temperature regions of the DSC features to move to higher temperatures. This increase in temperature causes a greater acceleration in the process with a higher activation energy. That the total exothermicity increases with temperature indicates that the exothermic channel has a higher activation energy as compared to that of the vaporization channel. In closed pan experiments, since no endothermic event except melting occurs before decomposition and the total heat release is largely independent of the heating rate (Figure 5), the contribution of the vaporization channel to the overall heat release would be expected to be minimal. As a result, the total heat release of 2250 J g^{-1} ($\sim$500 kJ mol^{-1}) should be mostly due to the exothermic decomposition channel. In open pan experiments the total heat release is about 5 times smaller as compared to that in closed pan experiments. The heat of vaporization of RDX can be estimated as the difference between the heats of sublimation (130 kJ mol^{-1} [31]) and fusion (36 kJ mol^{-1} [30]) that gives 94 kJ mol^{-1}. Using this value for the heat of vaporization, a branching ratio of decomposition to vaporization of 1 to 4 in open pans can be estimated. Therefore, in open pans most of the RDX undergoes vaporization despite the fact that the overall process is exothermic. The activation energy derived from open pan experiments is practically constant at $\sim$100 kJ mol^{-1} (Figure 4). This value agrees well with the above estimate for the heat of vaporization and also suggests that decomposition in open pans predominantly follows the endothermic vaporization channel.

As the endothermic channel appears to be significantly suppressed in closed pan experiments, the respective E_α dependence under these conditions should provide a good estimate for the activation energy for the exothermic decomposition channel. In a closed pan, the activation energy decreases from $\sim$200 to $\sim$135 kJ mol^{-1} (Figure 4), markedly greater than a value of $\sim$100 kJ mol^{-1} determined in open pan experiments and ascribed to the vaporization channel. This observation is consistent with the observed increase in the heat release with increasing heating rate in open and pierced pans and supports the exothermic decomposition channel having a larger activation energy than vaporization. The decrease in E_α from $\sim$200 to $\sim$135 kJ mol^{-1} suggests the presence of more than one decomposition channel in closed pan experiments. A plausible explanation for this decrease in the activation energy is decomposition of liquid RDX at early stages and an increasing contribution from decomposition of gas phase RDX at later stages of the overall decomposition. A contribution from gas phase RDX decomposition to the overall heat release was observed by Rogers and Daub,[22] which appeared as a small characteristic hump in isothermal DSC curves during the later stages of RDX decomposition. Separate kinetic analysis of this later part of a DSC curve allowed Rogers and Daub[22] to evaluate the activation energy of the gas phase decomposition as 143 kJ mol^{-1}, which is 54 kJ mol^{-1} lower than the value they determined, 197 kJ mol^{-1},[23] for liquid phase decomposition (Table 1). Data compiled by Brill et al.[32] from several studies also suggests that the gas phase decomposition of RDX has an activation energy that is about 60 kJ mol^{-1} smaller than for that in the liquid state. Therefore, a similar decrease in E_α in the present experiments likely reflects the transition of the rate-

limiting step from liquid state decomposition ($E_\alpha \sim$ 200 kJ mol^{-1}) to gas phase decomposition ($E_\alpha \sim$ 135 kJ mol^{-1}).

As would be anticipated, pierced pan experiments show behavior intermediate to open pan and closed pan experiments, including an appreciable contribution from the vaporization channel. The activation energies determined by isoconversional analysis for pierced pan experiments decrease from $\sim$160 to $\sim$135 kJ mol^{-1}, intermediate between the values determined for the exothermic decomposition and endothermic vaporization channels.

Thermogravimetric Analysis. Activation energies of $E_\alpha \sim$ 100 kJ mol^{-1} (Figure 4) determined by the isoconversional method for the first and major step of mass loss in open pan TGA experiments (Figure 1) are very similar to those determined in open pan DSC experiments; these values are both in good agreement with an estimated value of the enthalpy of RDX vaporization (vide supra). The abrupt decrease in E_α for $\alpha >$ 0.7 to $E_\alpha \sim$ 45 kJ mol^{-1} at $\alpha = 0.9$ and subsequent increase to $E_\alpha \sim$ 100 kJ mol^{-1} at $\alpha = 0.98$ coincides with the second mass loss step and may be due to the decomposition of a nonvolatile polyamide residue that has been observed previously.[1]

Several features of pierced pan TGA experiments (Figure 2) differ from those in open pans. The onset temperatures of all TGA traces collected in pierced pans occur above the melting point of RDX, i.e., when the sample is a liquid. The overall process shows a single stage of mass loss that exhibits a faster rate and a stronger temperature sensitivity relative to that in open pan experiments. A faster rate is observed as a sharper mass loss within a given trace. A stronger temperature dependence is evident in more closely spaced TGA traces as a function of heating rate that gives rise to a larger activation energy determined for the mass loss in a pierced pan. The activation energy for the process in pierced pans is fairly constant at $\sim$180 kJ mol^{-1} for $\alpha <$ 0.6, after which it decreases to $\sim$100 kJ mol^{-1}. The E_α dependence clearly differs from that obtained for pierced pan DSC experiments (Figure 4). The difference appears to be caused by the gas phase decomposition being detectable by DSC but not by TGA. In this case, the kinetics of the RDX decomposition observed in pierced pan TGA experiments should be determined by liquid state decomposition with $E_\alpha \sim$ 200 kJ mol^{-1} and vaporization with $E_\alpha \sim$ 100 kJ mol^{-1}. For this reason, the initial part ($\alpha <$ 0.6) of the E_α dependence demonstrates an effective activation energy that is somewhat lower than the activation energy for the liquid phase decomposition. The successive decrease in E_α at $\alpha >$ 0.6 appears to reflect the transition of the rate-limiting step from the liquid state decomposition ($E_\alpha \sim$ 200 kJ mol^{-1}) to vaporization ($E_\alpha \sim$ 100 kJ mol^{-1}). Further, the change from a two-stage mass loss in open pan TGA experiments to a single-stage mass loss in analogous pierced pan experiments suggest that while vaporization occurs early in open pans and later in confined environments, decomposition of a residue from RDX ($E_\alpha \sim$ 45$-$100 kJ mol^{-1}) participates in later stages in more open systems.

Previous literature reports and the data in the present TGA and DSC experiments suggest that the liquid state thermal decomposition of RDX involves three major steps: vaporization, liquid phase decomposition, and gas phase decomposition (Figure 6). The exothermic liquid state decomposition channel has an activation energy of $\sim$200 kJ mol^{-1}. A thin film laser pyrolysis study[3-5] strongly suggests that the initial step in the condensed phase decomposition of RDX is scission of an N$-$N bond. The latter is the weakest bond in the RDX molecule, and its dissociation energy of $\sim$200 kJ mol^{-1} (47.8 kcal mol^{-1})[33,34] is very similar to the activation energy for condensed phase
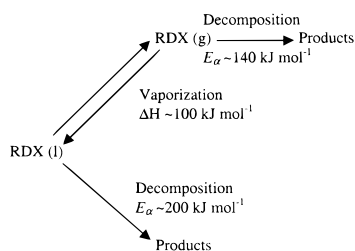
Figure 6. A kinetic scheme for the thermal decomposition of liquid RDX.

RDX decomposition determined in this study (vide supra). The vaporization of RDX can compete with condensed phase decomposition, is most prevalent in open pan experiments, and has an activation energy of $\sim$100 kJ mol^{-1}. The closed pan DSC results suggest that in a confined system, gas phase decomposition of RDX becomes important over the latter portion of the experiment and occurs with an activation energy of $\sim$140 kJ mol^{-1}. For the gas phase decomposition of RDX, both infrared multiphoton dissociation experiments in a molecular beam[35] and theoretical calculations[36,37] suggest a competition between N$-$N bond fission and concerted fission of three C$-$N bonds in the ring. The latter process is estimated[35-37] to have a lower energy barrier of around 150 kJ mol^{-1}, which gives rise to a branching ratio of $\sim$2 to 1 favoring ring fission. A surprisingly close value of the activation energy (140 kJ mol^{-1}) was estimated by Brill[38] for the decomposition channel leading to the formation of N_2O and CH_2O that was assumed to primarily occur in the condensed phase. However, because this estimate is based on the gas phase measurements of the N_2O/NO_2 concentration ratio, one cannot rule out the possibility for this channel to occur in the gas phase as well. Then the fact that the activation energy for this channel is very close to that of concerted fission of three C$-$N bonds suggests that the latter process may limit the formation of N_2O and CH_2O. On the other hand, the closeness of the values may simply be coincidental. At any rate, the results of the above-mentioned studies[33-37] provide viable explanations to the decrease in activation energy from $\sim$200 kJ mol^{-1} to $\sim$135 kJ mol^{-1} determined by isoconversional analysis of DSC traces of closed pan RDX samples.

Conclusions

The use of open, pierced, and closed pans for TGA and DSC experiments allows one to vary the contributions of condensed and gas phase processes in the overall rate of RDX decomposition. In open pan experiments the decomposition kinetics are primarily determined by vaporization. Conducting experiments in closed pans significantly suppresses vaporization and favors liquid state decomposition as the dominant process. Closed pan experiments show that gas phase decomposition of RDX also contributes during later stages of the decomposition ($\alpha \sim 1.0$). The isoconversional method reveals such competing processes in the heating of RDX because it can detect variations in the effective activation energy with the extent of RDX conversion. Analysis of open pan DSC and TGA experiments both yield activation energies that are fairly constant ($\sim$100 kJ mol^{-1}) throughout decomposition and are consistent with RDX vaporization. Both pierced and closed pan DSC experiments show a decrease in the activation energy with the extent of conversion

that is ascribed to a competition between liquid and gas phase decomposition. The initial stage of decomposition in closed pans has an activation energy of $\sim$200 kJ mol^{-1}, consistent with liquid phase RDX decomposition and which suggests scission of an N$-$N bond as a rate-limiting step. Close to completion, the activation energy drops to $\sim$140 kJ mol^{-1} due to an increasing contribution from gas phase decomposition. This decrease in the activation energy is most likely to reflect the transition of a rate-limiting step from N$-$N bond scission to concerted fission of three C$-$N bonds in the ring.

References and Notes

(1) Adams, G. F.; Shaw Jr., R. W. *Annu. Rev. Phys. Chem.* **1992**, *43*, 311.
(2) Brill, T. B.; James, K. J. *Chem. Rev.* **1993**, *93*, 2667.
(3) Botcher, T. R.; Wight, C. A. *J. Am. Chem. Soc.* **1992**, *114*, 8303.
(4) Botcher, T. R.; Wight, C. A. *J. Phys. Chem.* **1993**, *97*, 9149.
(5) Botcher, T. R.; Wight, C. A. *J. Phys. Chem.* **1994**, *98*, 5441.
(6) Ostmark, H.; Bergman, H.; Ekwall, K. *J. Anal. Appl. Pyrolysis* **1992**, *24*, 163.
(7) Brill, T. B.; Arisawa, H.; Brush, P. J.; Gongwer, P. E.; Williams, G. K. *J. Phys. Chem.* **1995**, *99*, 1384.
(8) Brill, T. B. *Anal. Chem.* **1989**, *61*, 897A.
(9) Brill, T. B. *Prog. Energy Combust. Sci.* **1992**, *18*, 91.
(10) Vyazovkin, S.; Wight, C. A. *J. Phys. Chem. A* **1997**, *101*, 8279.
(11) Vyazovkin, S.; Wight, C. A. *Int. Rev. Phys. Chem.* **1998**, *17*, 407.
(12) Vyazovkin, S. *Int. J. Chem. Kinet.* **1996**, *28*, 95.
(13) Vyazovkin, S.; Wight, C. A. *Annu. Rev. Phys. Chem.* **1997**, *48*, 125.
(14) Vyazovkin, S.; Wight, C. A. *J. Phys. Chem. A* **1997**, *101*, 5653.
(15) Vyazovkin, S.; Wight, C. A. *J. Phys. Chem. A* **1997**, *101*, 7217.
(16) Sell, T.; Vyazovkin, S.; Wight, C. A. *Combust. Flame* **1999**, *119*, 174.
(17) Robertson, A. J. B. *Trans. Faraday Soc.* **1949**, *45*, 85.
(18) Bawn, C. E. H. *Chemistry of the Solid State*; Butterworth: London, 1955; p 254.
(19) Rogers, R. N.; Morris, E. D. *Anal. Chem.* **1966**, *38*, 412.
(20) Rauch, F. C.; Fanelli, A. J. *J. Phys. Chem.* **1969**, *73*, 1604.
(21) Hall, P. G. *Trans. Faraday Soc.* **1971**, *67*, 556.
(22) Rogers, R. N.; Daub, G. W. *Anal. Chem.* **1973**, *45*, 596.
(23) Rogers, R. N. *Thermochim. Acta* **1974**, *9*, 444.
(24) Kishore, K. *Propellants Explos.* **1977**, *2*, 78.
(25) Kishore, K. *Anal. Chem.* **1978**, *50*, 1079.
(26) Oyumi, Y. *Propellants Explos. Pyrotech.* **1988**, *13*, 42.
(27) Kissinger, H. E. *Anal. Chem.* **1957**, *29*, 1702.
(28) Galwey, A. K.; Brown, M. E. *Thermal Decomposition of Ionic Solids*; Elsevier: Amsterdam, 1999.
(29) Vyazovkin, S. *J. Comput. Chem.* **1997**, *18*, 393.
(30) Meyer, R. *Explosives*, 3rd ed.; VCH: Weinheim, Germany, 1987.
(31) Rosen, J. M.; Dickinson, C. *J. Chem. Eng. Data* **1969**, *14*, 120.
(32) Brill, T. B.; Gongwer, P. E.; Williams, G. K. *J. Phys. Chem.* **1994**, *98*, 12242.
(33) Melius, C. F.; Binkley, J. S. *Proc. 21st Int. Symp. Combust.* **1986**, 1953.
(34) Melius, C. F. In *Chemistry and Physics of Energetic Materials*; Bulusu, S. N., Ed.; Kluwer: London, 1990.
(35) Zhao, X.; Hintsa, E. J.; Lee, Y. T. *J. Chem. Phys.* **1988**, *88*, 801.
(36) Sewell, T. D.; Thompson, D. L. *J. Phys. Chem.* **1991**, *95*, 6228.
(37) Chambers, C. C.; Thompson, D. L. *J. Phys. Chem.* **1995**, *99*, 15881.
(38) Brill, T. B. *J. Propuls. Power* **1995**, *11*, 740.